Geotech Geol Eng
https://doi.org/10.1007/s10706-024-02859-5

ORIGINAL PAPER

Discontinuity-Induced Partial Instability in Markundi Hills, Sonbhadra, Uttar Pradesh, India

Vikas Yadav · Ashutosh Kainthola · Vishnu H. R. Pandey · Gaurav Kushwaha · T. N. Singh

Received: 12 April 2024 / Accepted: 14 June 2024

Abstract State Highway-05A in Northern India, connects the states of Chhattisgarh, Madhya Pradesh, Uttar Pradesh, and Jharkhand. In Uttar Pradesh, it passes through steep and rugged Markundi Hill, composed of highly jointed sandstone. The current study examines road-cut slopes at six locations to quantify the instability mechanism and slope health. Detailed field and laboratory investigations were combined to ascertain the structural, petrographic, and strength attributes of the rock. Afterwards, data was collated to characterise the rockmass behaviour through widely accepted classification schemes, viz., geological strength index (GSI), Q-slope, rock mass rating (RMR), slope mass rating (SMR), and modified global slope performance index (modified GSPI). The value ranges provided by various empirical classifications are 40–62 (RMR), 39.61–58.46 (SMR) and modified 44.57–52.57 (GSPI). For structural stability, kinematic analysis was conducted. According to RMR, five locations fall in fair and one in poor rockmass classes. SMR suggest all locations are partially stable. Eventually, a novel approach for finding the ratings of GSPI is also introduced in the present work, allowing more comprehensive discontinuity characteristics incorporation. The new approach brings GSPI and SMR to the same scale, making it easy to compare the two. GSPI yields that all the locations have high chances of local bench failures. Compared to other approaches, GSPI predicts a wide range of instabilities and should be used alone or in conjunction with other systems for slope stability assessment.

Keywords Rockmass classification schemes · Geological slope performance index · Slope stability · Markundi hill

V. Yadav · A. Kainthola (✉) · V. H. R. Pandey · G. Kushwaha
Department of Geology, Banaras Hindu University, Varanasi 221005, India
e-mail: ashutosh.geo@bhu.ac.in

V. H. R. Pandey
Dipartimento di Scienze della Terra, "Sapienza" Università di Roma, Piazzale Aldo Moro, 5, 00185 Rome, RM, Italy

T. N. Singh
Indian Institute of Technology, Patna, Patna 801106, India

1 Introduction

The roadways are vital arteries for all socio-economic well-being of a nation, thus safety along the hill-slopes is a major concern for the administration. Up until the last century, mountains were not connected well with mainstream cities and hence were devoid of development and economic activities (Kainthola et al. 2023). In recent decades, with the activities of engineering construction vis-a-vis climate change, the degradation of hilly regions due to erosion of soil, and landslides is a result (Li et al. 2024). Slope instability is a major concern affecting the health and

Published online: 28 June 2024

functioning of the economic projects in the mountains (Chand and Koner 2024). Discontinuity-induced partial instability are often displayed in these environments. Many researchers have analyzed the influence of joints on the failure mode of surrounding rock in this perspective (Peng 2024). Thus, a detailed understanding of the geotechnical and geological attributes of rock masses is incorporated in planning mega projects (Dikshit et al. 2020; Monjezi and Singh 2000; Rawat et al. 2024). However, an accurate and reliable estimation of stability is challenging. Slope stabilization methods are possible with specific skills, but must include a comprehensive study in a realistic way (Gordan et al. 2015). Various methods exist for stability and safety estimation—with their assumptions and approximations. The inherent property of rocks has a dominating control over the stability of the slopes, which is also influenced by exogenic processes of the earth and anthropogenic activities (Yoon et al. 2002). In this respect, rockmass characterization and comprehension of slope failure behavior aid the implementation of economic and robust protective actions (Bartarya and Valdiya 1998; Starkel 1972; Virdi et al. 2015). Determination of stable angles of cut-slope and excavation practices are essential for the development of highways in hilly regions (Avcı et al. 1999). Evaluation of discontinuity condition aids in the comprehension of slope stability assessment and support requirements (Sardana et al. 2019). Kinematic analysis is a handy method to find allowable moments of the joint sets considering the orientation of the slope and the angle of internal friction along the discontinuity plane (Rahman et al. 2023). Also, the joint conditions including roughness, persistence, aperture, spacing, fillings, etc., joint roughness coefficient (JRC), joint compressive strength (JCS), and water movement along them have a crucial role in stability (Singh and Monjezi 2000; Monjezi et al. 2011). Doumbouya et al. (2020) finds rainfall infiltration is the enabler for initiating the failure of the upper slope at Malundwe open pit. For many civil and mining engineering structures such as road cut, rockmass is the primary construction medium and mechanical behavior of a rockmass is defined by attributes of its intact rock (West 2024). Thus, discerning the various geotechnical features of the intact rocks through laboratory testing is an imperative for slope stability calculation. To attain this, a series of different field and laboratory test were executed. The Rebound Hammer is a convenient tool to enumerate the indirect strength of the rock in the field (Brencich et al. 2020). Point load index test, Brazilian test, and uniaxial compressive strength (UCS) can be conducted in the laboratory to measure different types of strengths. Also, to understand the effect of weathering, slake durability (Franklin and Chandra 1972) tests are routinely performed.

Rockmass classification schemes are the means of quickly assessing the performance of slope and underground excavations (Hassan and Hani 2017). Azarafza et al. (2022) stated that the preliminary responses on stability assessment are very effective in discontinuous rock slope stabilizations which can be done by geo-mechanical/empirical approaches. Several rock mass classification systems are industrialized for rock cuttings with high risk to ascertain their failure possibility and preventive measures (Ansari 2019). Rock Quality Designation (Deere 1963), Rock Mass Rating (Bieniawski 1979, 1989), Geological Strength Index (Hoek et al. 1995; Hoek and Brown 1997; Marinos and Carter 2018), Slope Mass Rating (Romana 1985, 1993), Q-Slope (Barton and Bar 2015), and Geological Strength Performing Index (Sullivan 2013) are some of the pertinent classification schemes. Several researchers have done assessments of slopes by using these established empirical approaches (Das et al. 2024; Chaudhary et al. 2022; Tiwari et al. 2020; Kainthola et al. 2021; Pandey et al. 2022; Panthee et al. 2023). Kinematic analysis is a conventional method for slope stability utilized in this work (Rahman et al. 2023). These are restricted to basic difficulties in their range of application, covering simple geometries of the slope and primary loading conditions and they provide less highlight into slope failure mechanisms (Eberhardt 2023). State Highway-05A, is an important roadway connecting the Indian State of Uttar Pradesh to the neighbouring States. The sections near Markundi Ghats (SH-05A) are hilly and witnesses frequent failures. Therefore, a thorough geotechnical examination of rockmass and slopes around Markundi Hill is essential to avert & mitigate mishaps. All geotechnical parameters required for empirical stability analysis were analyzed through standard laboratory testing. Q-Slope, GSI, RMR, SMR, and GSPI were employed for characterization and stability classification. A new approach to calculating GSPI is introduced in this article by borrowing a few parameters from SMR. These are the two most weighted parameters of RMR namely spacing of discontinuities and condition of discontinuities. The main application of this approach is to compare the GSPI with robust classification like SMR at the same scale.

2 Study Area

The study area is the chunk of Markundi Hills of Sonbhadra district, Uttar Pradesh, India. Geologically, it belongs to the Upper Group of Kaimur of the Vindhyan Supergroup (Kumar et al. 2019). The area under investigation is bound between the latitude of 24°37′12.33'' N to 24° 37′ 8.58'' N and the longitude of 83°2′40.33'' E to 83° 2′ 11.832" E (Fig. 1). The Vindhyan supergroup consists of carbonate, sandstone, and shale with a marginal amount of conglomerate and volcano-clastic beds. Scarp and Dhandraul sandstones of the Kaimur Group are the main rocks in the study area (Mishra and Sen 2011). Markundi Hill is dissected by the Jamui-Markundi fault (a reverse fault) along with several other small-scale faults. The study area lies over faults that make the hill susceptible to failure. Topographically, the hill is steep and dipping southward with rugged/ undulating terrain (Kumar et al. 2019). Widening activities by mechanical excavation and blasting, exposes the joints on the slope, rendering them more susceptible to weathering. Presently, data and samples were taken from six critical slope sections, named L-1 to L-6 (Figs. 1 and 2). Figure 3a shows location 1 which is mostly made up of quartz and muscovite. Figure 3b and c represents locations 2 & 6 respectively, which are also mostly made up of quartz and muscovite. Muscovite is present mainly as interstitial grain and cementing material. As a whole, very abundant monocrystalline quartz grains in a micaceous matrix are present. Micaceous minerals exhibit bending and alignment parallel to the lamination of sandstone (Fig. 3).

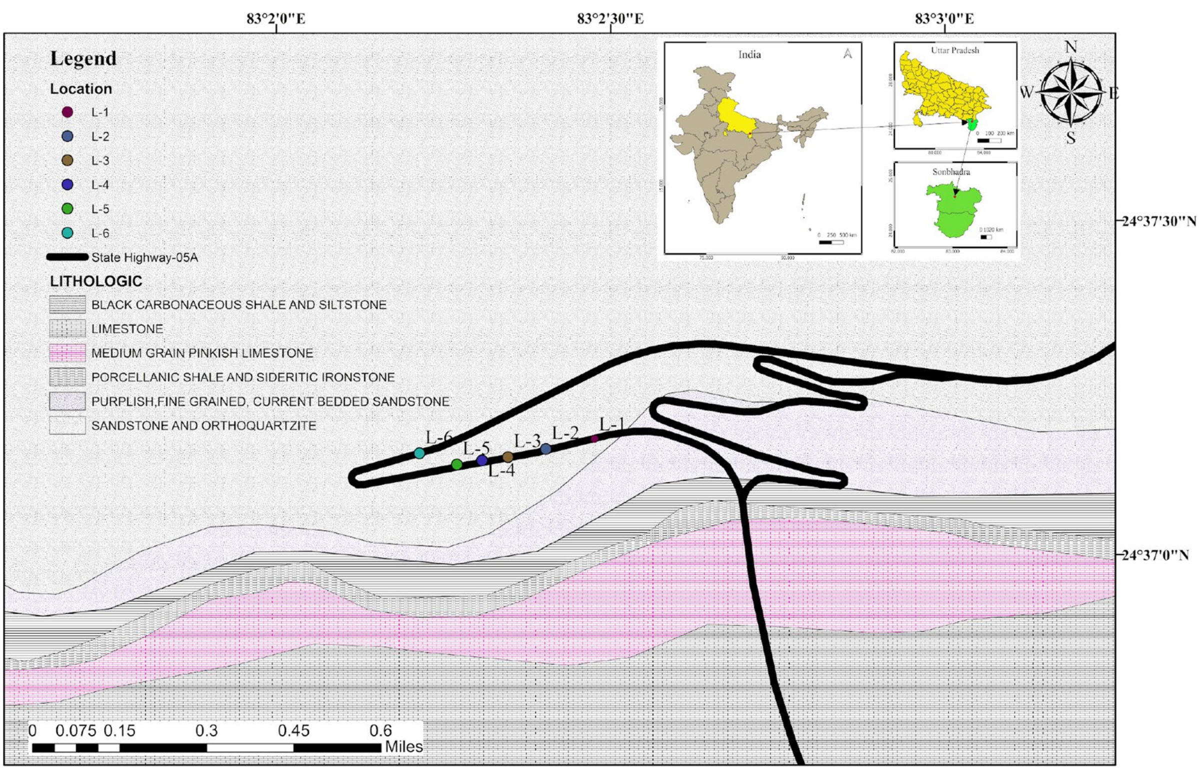

Fig. 1 Geological map of the Markundi Hill (Geological Survey of India 2023)

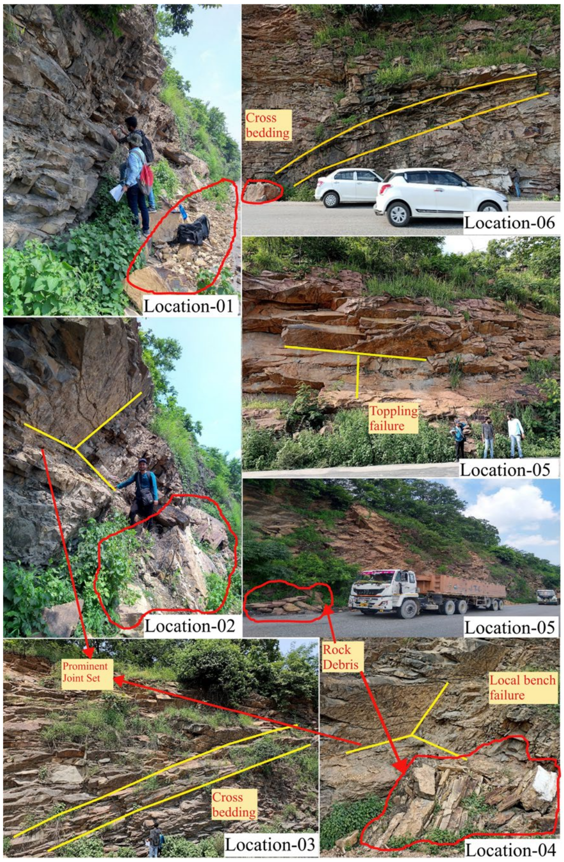

Fig. 2 Field photographs of the study area

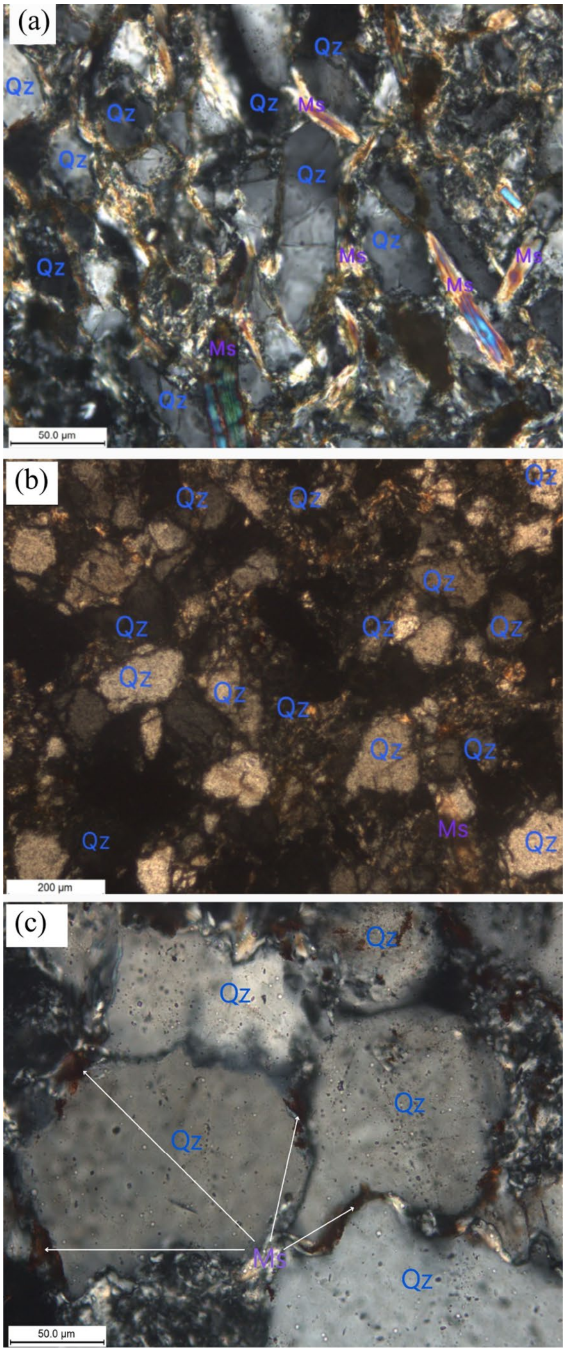

Fig. 3 Microscopic images of the samples, where Qz represents quartz and Ms is muscovite **a** location-01, **b** location-02, **c** location-06

3 Methodology

Rockmass classification schemes require detailed field investigation and laboratory data as inputs. During field investigation, several discontinuities, spacing, condition of discontinuity, and orientation of slope were recorded. Kinematic analysis needs field data and the angle of internal friction of the discontinuity plane for the prediction of the type of failure. Samples were picked for detailed research and laboratory testing. In the lab, the strength of the intact rocks, deformation modulus, and weathering index were calculated. These parameters were used as input parameters to characterize the rockmass. Eventually, rockmass classifications and kinematic analysis were performed to understand the behaviour and stability of the rockmass at different locations (Fig. 4).

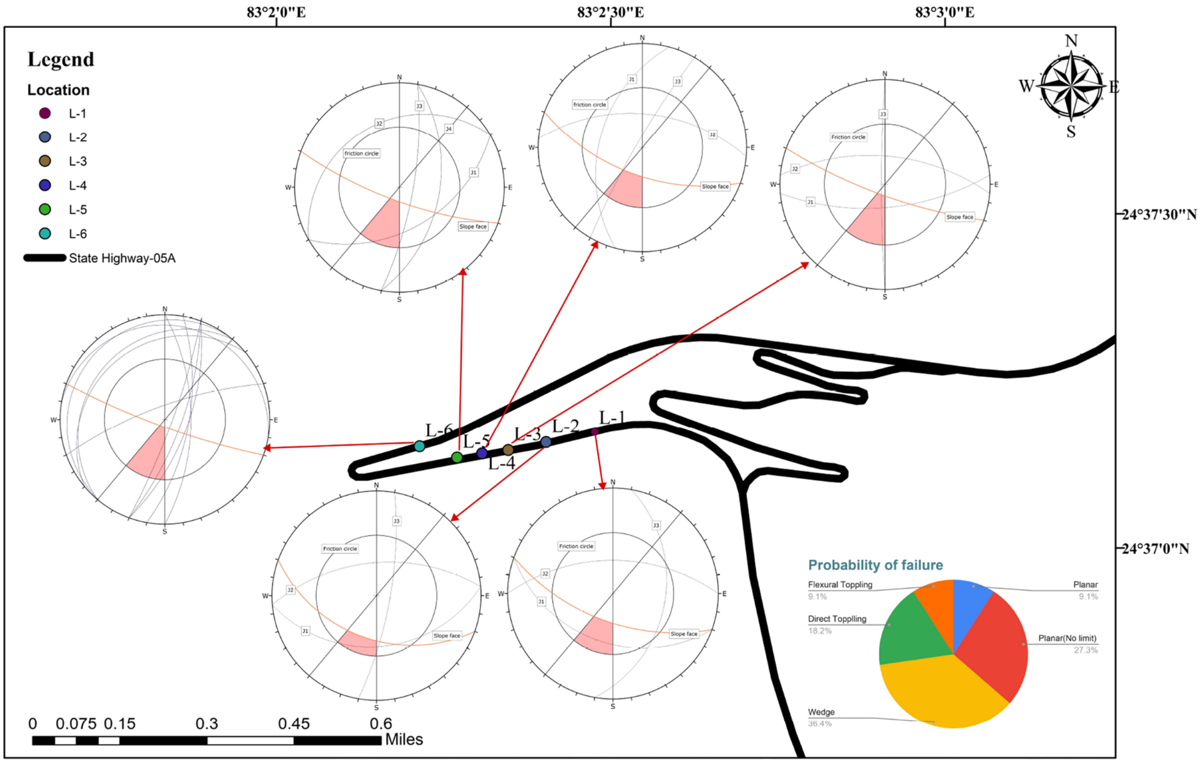

Fig. 4 Engineering geological map of study location

3.1 Laboratory Investigation

Different geotechnical laboratory tests require a specified sample size (Fraser-Harris 2020). To assess the geotechnical parameters of the Markundi sandstones, ample representative samples were collected from critical sections. NX-size cores following ISRM/ASTM guidelines were extracted for different physico-mechanical tests. Approximately, 50 core samples were prepared from the collected rock specimens using diamond core drill bits (Fig. 5a). For the point load index (PLI) test, the samples with dimensions L/D > 0.5 for diametral tests and 0.3W < D < W for axial tests were considered. For the slake durability test, 10 small pieces of samples containing (40–60) g each were prepared for all target locations.

3.2 Rebound Hammer Strength Test

A rebound hammer provides a swift measure of surface hardness that is used for approximating the mechanical properties of rocks (Aydin and Basu 2005). In the field investigation Rebound hammer data has been taken for each location in all three possible directions. i.e. downward, upward, and horizontal depending on the joint surface exposed.

3.3 Point Load Index (PLI)

The point load test consists of loading the rock sample with two-pointed hardened steel cones based on the principle that tensile stress into the rock can be generated by compression of rock (Norbury 1986). It is an index test for the estimation of the strength of intact rock masses (Broch et al. 1972). In the present work, both diametral and axial tests were accomplished over rock cores (Eqs. 1 and 2).

$$I_S = \frac{P}{{D_e}^2} \tag{1}$$

$$\text{where, } D_e = \sqrt{\frac{4A}{3.14}},\ and\ A = W * D$$

$$\sigma_c = K * I_S \tag{2}$$

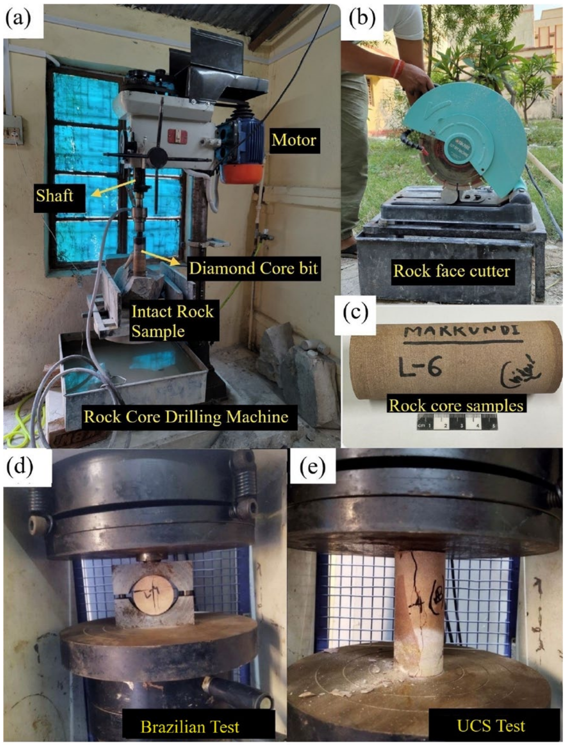

Fig. 5 **a–c** Rock core sample preparation from intact rock. **d** & **e** Brazilian and UCS test

where, I_S = Uncorrected point load strength, P = Peak failure load, W = Width, D = Diameter, D_e = Equivalent core diameter. For the scarp sandstone of the Markundi hill $K = 24$ was considered.

3.4 Brazilian Test

The Brazilian test is an indirect method to discern the tensile strength of the rock. The sample required for the test should be of NX size core and the L/D ratio must be between 0.2 and 0.75, generally half of the diameter (Eq. 3).

$$\sigma_t = \frac{2P}{\pi * D * t} \tag{3}$$

where, σ_t = Tensile strength, P = Failure load, t = Thickness of the sample, D = Diameter of the sample.

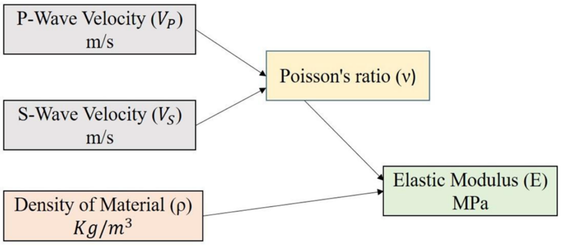

Fig. 6 Schematic for calculation of Poisson's ratio and elastic modulus

3.5 Uniaxial Compressive Strength (UCS), Elastic Modulus, Poisson's Ratio and P-Wave Velocity

Young's modulus (E) is a fundamental geo-mechanical parameter commonly utilised in rock engineering applications. It is typically determined through a uniaxial compressive strength (UCS) test (Małkowski et al. 2018). UCS was determined as per the protocols laid by ISRM. P-wave and S-wave were measured by Pulse velocity testing equipment to ascertain the Poisson's ratio and Young's modulus (Fig. 6). Equation 4 (Aki and Richards 2002) and Eq. 5 (Shearer 2009) were employed for the calculation.

$$v = \frac{V_p^2 - 2V_s^2}{2(V_p^2 - V_s^2)} \tag{4}$$

$$\mathrm{E} = 2\rho V_s^2 (1 + v) \tag{5}$$

where V_p & V_s are the primary and secondary velocity respectively, v is the Poisson's ratio and E is the elastic modulus.

3.6 Slake Durability Test

The slake durability test processes the degree of resistance offered by a rock sample to exposure to the drying and wetting cycle (Franklin and Chandra 1972). A total weight of approximately 450 g consisting of 10 rock pieces each weighing 40–60 g are taken in this experiment. ISRM standard was followed for the test.

4 Rockmass Characterization

4.1 Geological Strength Index (GSI)

GSI was given by Hoek and Brown (1997) and improved by different workers (Marinos and Hoek 2000; Sonmez and Ulusay 2002). GSI quantifies the overall geotechnical quality of the rocks and it determines the qualitative value of blockiness in rockmass at a scale ranging from 0 to 100 (Hong et al. 2017). All six locations in the study area were evaluated for GSI during the field investigation (Fig. 7).

4.2 Q_{slope}

Q_{slope} is a quick and tangible empirical approach to evaluate slope stability at the site of construction and allows the desired adjustment in the slope angle (Bar and Barton 2017). Modified after the Q-value, it is used to give the maximum angle of the unreinforced excavated slope (Eq. 6). Q-slope vs slope angle vis à vis stable slope angle for Markundi Hills is represented in Fig. 8.

$$Q_{Slope} = \frac{RQD}{J_n} \times \left(\frac{J_r}{J_a}\right)_0 \times \frac{J_{wice}}{SRF_{Slope}} \tag{6}$$

where, J_n represents the number of joint sets, J_r is the joint roughness number, J_a is the joint alteration, J_{wice} is an environmental effect, and SRF is the slope stress reduction factor.

4.3 Rock Mass Rating (RMR)

RMR classifies the rockmass into several classes, based on simple parameters, to evaluate and suggest adequate support systems for excavation projects (Bieniawski 1976). Initially, five parameters were used to characterize the rockmass, referred to as RMR_{basic}. These attributes were UCS, RQD, spacing of discontinuities, condition of discontinuities, and groundwater conditions. However,

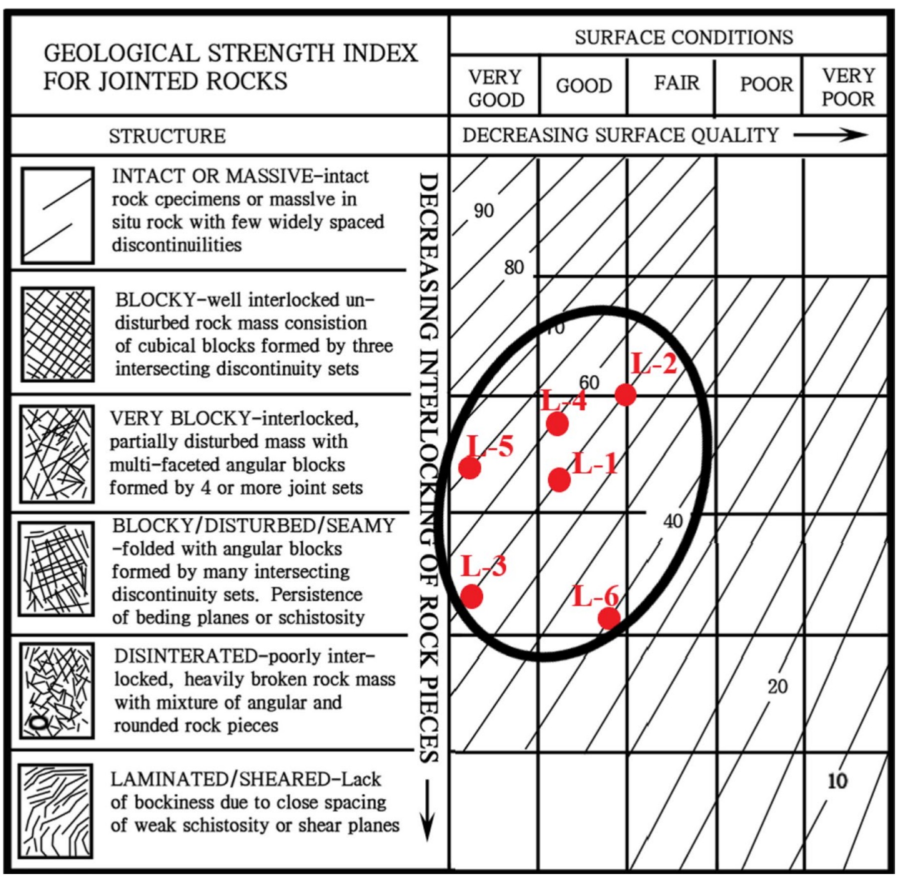

Fig. 7 GSI classification of rockmass along Markundi cut slopes (after Hoek and Brown 1997)

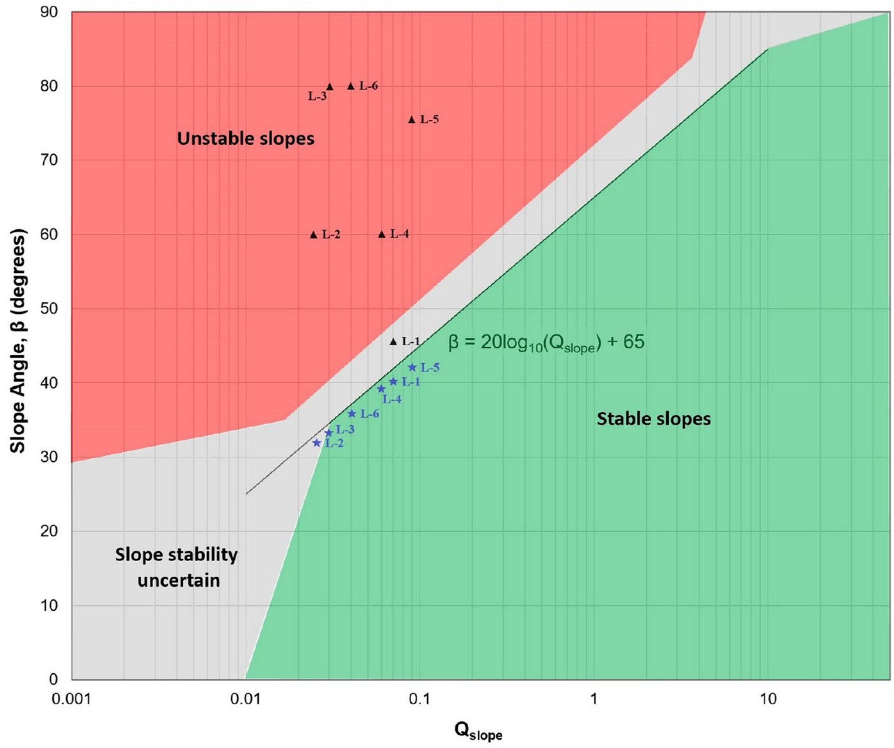

Fig. 8 Q_{Slope} versus the slope angle for studied Markundi Hill slopes (after Bar and Barton 2017)

based on various field data and practical judgment another important attribute "joint orientations" was incorporated to make a diligent decision (Bieniawski 1989).

Deere (1963) coined a quantitative approach of Rock Quality Designation (RQD) to acknowledge rockmass condition-based frequency of joints along a direction (Eq. 7). Generally, RQD is the percentage index demarcating the rock mass quality from very poor to excellent.

$$RQD(\%) = \frac{\Sigma(Length\ of\ core\ pieces) \geq 0.10m)}{Total\ length\ of\ core\ run} * 100 \tag{7}$$

Palmstrom (1974) has correlated RQD with volumetric joint count (Eq. 8).

$$\mathrm{RQD} = 115 - 3.3\mathrm{Jv} \tag{8}$$

where, J_v refers to the volumetric joint amount of the rockmass. $J_V = \frac{1}{S_1} + \frac{1}{S_2} + \frac{1}{S_3} + \ldots,\ S_1, S_2, S_3, \ldots$ are the joint spacing. The Markundi slopes are dry in general however signs of water at some locations are observed during the site investigation.

4.4 Slope Mass Rating (SMR)

SMR is a very well-accepted rock mass classification scheme used to evaluate the health of the slope (Romana 1985, 1993). SMR is obtained by introducing four adjustment factors F_1, F_2, F_3, and F_4 in addition to the RMR_{basic} (Eq. 9).

$$\mathrm{SMR} = \mathrm{RMR_{basic}} + (\mathrm{F1.\ F2.\ F3}) + \mathrm{F4} \tag{9}$$

where, F1 denotes the correlation between the direction or strike of the joints and slope, F2 characterizes the gradient or inclination of the slope, F3 depicts the relation between the dip of the joints and the steepness or dip of the slope and F4 depends on excavation techniques (Goel and Singh 2011).

4.5 Global Slope Performance Index (GSPI)

GSPI integrates five indices viz., the strength of intact rock, rockmass character, geological structure, and the orientation of structures concerning slope orientation, and response patterns of groundwater and its conditions (Sullivan 2013). Attributes like geological structures, intact strengths, and groundwater conditions contribute significantly to the stability of the slopes (Chiwaye and Stacey 2010). The geological structure has three sub-parameters—rockmass character, the orientation of the structure, and the type of controlling structure (bedding plane, joints, folds or faults, etc.). Intact strength is widely accepted in all classification schemes because of its importance. Unlike the Global slope performance index, RMR, SMR, or either Q-System doesn't consider geological structure as a parameter. The presence of folds, faults, and bedding planes parallel to the slope face highly influences the health of the slope (Rehman et al. 2023). SMR is calculated with six parameters of unequal importance, whereas GSPI depends on five parameters of all equal importance. In comparison, the strength of the rock, RQD/GSI, groundwater conditions, and the relationship between discontinuities & slope orientation are common parameters in both classification schemes. The different parameters are spacing and condition of discontinuity from SMR and geological structure from GSPI. The presence of discontinuity on the slope face affects the slope instability (Hoek and Bray 1981). Aperture, persistence, roughness, type of infilling, and degree of weathering of the discontinuities altogether influence slope stability (Shang et al. 2018). Depending on their conditions it cannot be ignored.

For a better understanding of slope performance, the authors introduce a new approach to calculating the GSPI score. By adding the different parameters from the very well-accepted and documented rockmass classification scheme such as SMR in the original GSPI scheme. In the SMR, condition and spacing of discontinuity have a weightage of 50% of the total rating, making them the most important parameters. Hence these parameters have been used in the new GSPI scheme along with its five original parameters. The author rated these parameters following the norms given by (Romana 1985, 1993), and by normalizing, it will be used in modified GSPI. In the GSPI, parameters vary on the scale of 1–5 and the total sum is a maximum of 25, but in the modified rating each parameter is to make the sum of 100 likewise SMR. Now, all the existing parameters will vary on the scale of 2.4–12 multiplying the conversion factor of 2.4 in all five parameters individually. Ratings of each parameter will be done based on Sullivan (2013). Parameter-like spacing of discontinuity discussed in SMR varies on the scale of 5–20 in SMR and will remain as in modified GSPI. Conditions of discontinuity vary on the scale of 0–30 in SMR and are made to vary on the scale of 0–20 in the modified GSPI followed by a conversion factor of 0.67. Rating is centered on the description of (Romana 1985, 1993) in SMR. Both the conversion factors have been calculated using the law of ratio and proportionality. The sum of all five parameters in the original GSPI scheme is 60 and the two parameters borrowed from the SMR is 40, making a total of 100. The borrowed parameters from SMR are given 40% weightage because of their high influence on the stability of the slope. Parameters of modified GSPI Classification and their ratings are given in Table 1.

5 Kinematic Analysis

Depending on the rock/soil type, and discontinuity orientation, four types of failures, i.e. wedge, planar, toppling, and circular instabilities can take place (Fig. 9). Kinematics of failure are governed by the orientation of discontinuity, slope face, and angle of internal friction (Park et al. 2015).

For the present work, all the studied slope sections were analyzed for stability under different geometric conditions.

6 Results and Discussion

The road cuts, with varying slope heights, provided optimal exposure for assessing lithological variations, weathering conditions, and structural features, as well as recording joint patterns for rock excavation purposes. Three and some random joints were present, as shown in Fig. 4. The bedding plane and slope are almost parallel to each other, along the road stretch, causing planer failure that was observed at location 5 (Fig. 2). Local bench failure was observed at all the locations except location 6. Rockmass faces were stained and had clay infillings along different joint sets expressing moderate weathering conditions. Location 6 is highly jointed having numerous joint sets. Rockfalls were prominent and water seepage was also present. Along the road-cut, two formations namely Dhandraul sandstone at the top and Mangesar formation (Scarp sandstone) are exposed near the

Table 1 Parameters of modified GSPI Classification and their ratings

Parameters		Range of values				
Parameters of modified GSPI Classification and their ratings						
1	Strength of intact rock UCS (MPa)	< 5	5–25	25–50	50–100	> 100
	Rating	2.4	4.8	7.2	9.6	12
2	Rock mass character	Massive	Blocky	Very blocky	Disrupted, exhibiting substantial folding and/or faulting	Altered, subjected to shearing, and/or characterized by intense lamination or foliation
	Rating	2.4	4.8	7.2	9.6	12
3	Geological structure	Joints	Jointed	Foliated/Bedded/Contacts/unconformities	Alteration Zones/Shears	Faults
	Rating	2.4	4.8	7.2	9.6	12
4	Alignment concerning the excavated slope					
	Dip	Into slope, < 50°	Parallel, ± 10°	Out of slope 0 to 5°	Out of slope 5° to 20° Into slope 50° to 80°	Out of slope, > 20°
	Strike	Into slope, > 15°	Parallel to slope ± 0° to 30°	Parallel to slope ± 0° to 45°	Parallel to slope ± 5° to 20° Parallel to slope ± 0° to 15°	Parallel to slope ± 0 to 25
	Rating	2.4	4.8	7.2	9.6	12
5	Groundwater condition	Dry	Low	Moderate	Elevated	Highly to fully saturated
	Rating	2.4	4.8	7.2	9.6	12
6	Spacing of discontinuities	> 2 m	0.6–0.2 m	200–600 mm	60–200 mm	< 60 mm
	Rating	20	15	10	8	5
7	Condition of discontinuities	Very rough surfaces, not continuous, no separation, Unweathered wall rock	Slightly rough surface, Separation < 1 mm Slightly weathered walls	Slightly rough surface, Separation < 1 mm Highly weathered walls	Slickenside surfaces Or Gouge < 5 mm thick Or Separation 1–5 mm continuous	Soft Gouge > 5 mm thick Or Separation > 5 mm continuous
	Rating	20	16.67	13.33	6.66	0

road section. Framework grain is mostly quartz surrounded by micaceous matrix as shown in Fig. 3. In-situ, intact strength has been obtained from Rebound Hammer using rebound numbers. UCS value varies depending on the applied direction. Since rock consists of various strengths, the average value of the USC by Rebound Hammer displays maximum in a downward direction, intermediate in horizontal, and minimum in a vertical direction for the same intact rocks (Fig. 10). The lowest variation in the strength is shown by location 1 and maximum variation was observed at location 6 on taking measurements in different directions.

The point load index (PLI) value is used to predict indirect UCS strength in the directions of axial and diametral on a cylindrical core. PLI (axial) > PLI (diametral) for each rock sample of the study area. Uniaxial compressive strength ranges between 30

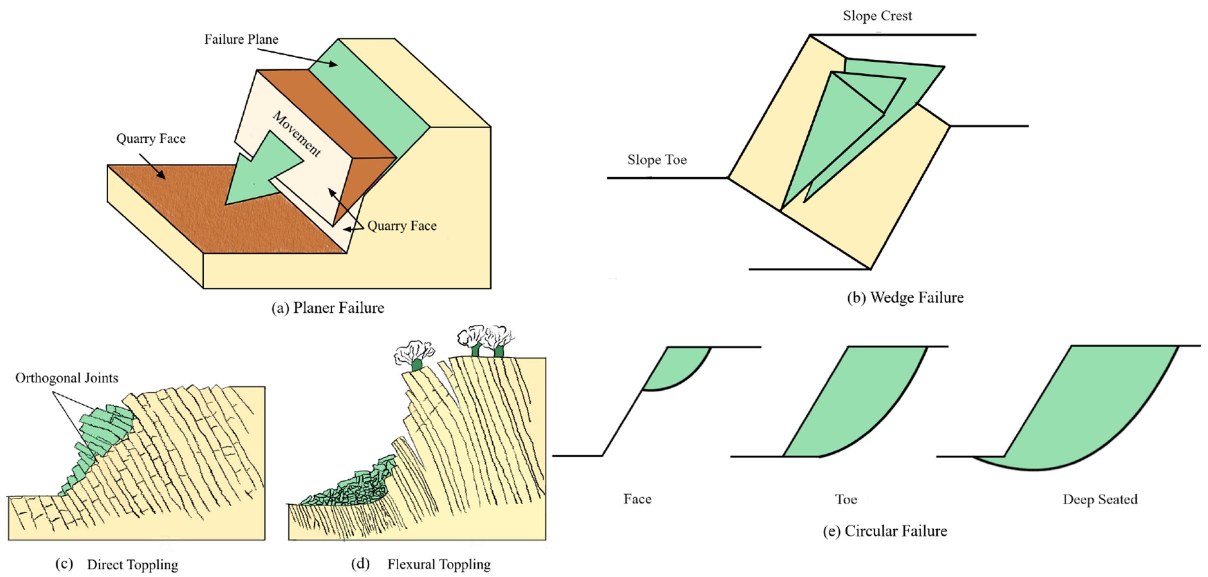

Fig. 9 Types of slope failure; **a** planar, **b** wedge, **c** & **d** toppling, **e** circular (Hoek and Bray 1981)

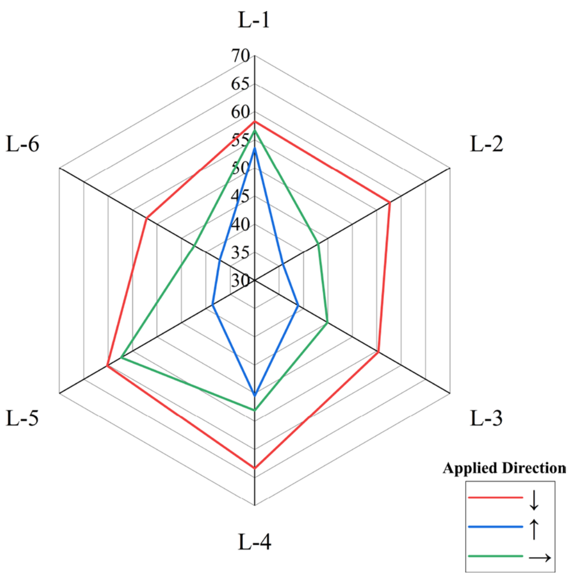

Fig. 10 Compressive strength of the intact rock by Rebound Hammer

and 91 MPa, which falls into the moderately strong to strong classes (Table 2). Locations 1, 2 and 3 have almost similar and low UCS values compared to locations 4, 5 and 6. Sandstone was present at all the locations having variable clay content. As the clay content decreased along the road from the L-1 to L-6, strength increased. As shown in Fig. 3, it is visible that location 6 has larger quartz grains and lesser matrix, compared to locations 1 and 3, hence its strength shows variations. The tensile strength of the rock lies between 8.04 and 12.58 MPa (Table 2). The samples collected from location 4 yield maximum strength followed by location 5, whereas locations 1, 3 & 6 have distinct and uneven values showing variable strength. Location 2 is characterized as a uniform and weak rock because it shows very less and approximately the same value for all types of tests (Fig. 11). P-wave velocity readings were similar for locations 1–5 and lowest for location 3. P-wave velocity for Markundi sandstone varies from 3189 to 3943 m/s, Poisson's ratio from 0.23 to 0.26, and Young's modulus from 22.06 to 34.14 GPa. Poisson's ratio was calculated with the help of P-wave velocity instruments. There is very little variation in the Poisson's ratio for all locations and ranges of 0.22–0.26. Young's modulus follows a similar trend of p-wave velocity. Based on Poisson's ratio and Young's modulus, the scarp sandstone of Markundi Hill is moderately hard sandstone (Molina et al. 2017). Slake durability index is measured around 96.49–98.83%.

The geological strength index was calculated in the field itself for all locations from the chart given by Hoek and Brown (1997). Location 3 & 6 have very good and good surface quality respectively (Fig. 7).

Table 2 Detailed geotechnical testing results

Location	PLI-UCS (Axial)	PLI-UCS (Diametral)	UCS	Strength by Rebound	Brazilian (Tensile)	P-Wave Velocity (m/s)	Poisson's Ratio	Young modulus (GPa)
L-1	65.19	41.57	47.34	51.78	8.45	3348	0.24	25.37
L-2	41.21	32.38	39.48	45.47	10.03	3202	0.23	24.09
L-3	83.40	35.68	30.55	46.36	8.08	3189	0.22	22.06
L-4	137.91	73.60	91.17	55.59	12.58	3478	0.25	26.24
L-5	96.99	60.98	74.67	53.52	9.45	3256	0.23	23.48
L-6	94.42	55.76	73.65	52.13	8.04	3943	0.26	34.14

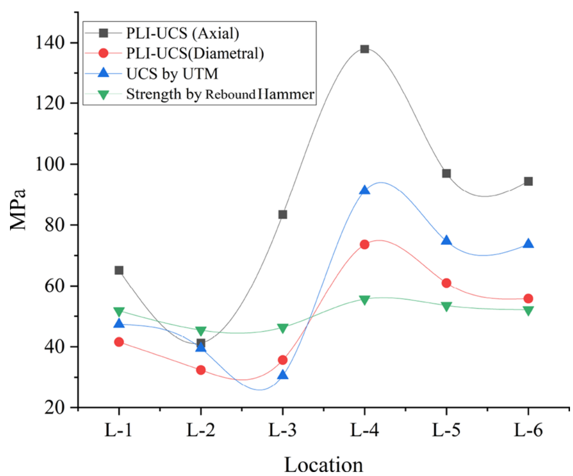

Fig. 11 Comparison of Compressive strength value at different testing techniques

It contains a highly blocky/disturbed rock structure folded with angular blocks created by numerous intersecting sets. Location 5 has very good surface quality and locations 1, 2, & 4 have good surface quality with highly blocky, interlocked, partially disturbed masses with multi-faceted angular blocks formed by four or more sets of joints.

According to Q-slope location 1 is at the boundary of stable and unstable slope conditions, and all the remaining slopes are unstable. In detail, the Q-Slope values interpret that most of the location lies outside the stability range. The relationship between Q-slope and slope angle is in detail in Fig. 8.

The hill-slopes are characterized by the RMR (1989) classification. However, the majority of SMR values for the road section fall under class III, which is partially stable having a probability of failure value of 0.4 (Romanna 1985). Also, for the first time, GSPI is introduced to the Vindhyan rockmass for evaluating slope stability performance along the Markundi Ghats (Table 1). The new approach to calculating GSPI can conclude the SMR results and can be compared with other popular rockmass classification schemes at a scale of 100. Additionally, based on SMR the most unstable location is L-6, belonging to the SMR class IV a, with a 60% probability of failure and the rockmass condition is bad (Romana 1985). All the remaining locations belong to class III where the probability of failure is 40% (Romana 1985). Locations 2, 3 & 5 belong to IIIa, and locations 1 & 4 belong to IIIb. According to the modified GSPI, all the locations fall in class III and will have local bench failure which can be seen in Fig. 12 at location 4. During our field visit, multiple bench failures along the slope were observed that verified the findings from the modified GSPI. Results of SMR and modified GSPI show a very good correlation as the slopes at all the locations show the same type of failure pattern in both the classification schemes (Fig. 13). Orientation of the discontinuity on the slope face, and steep slope angles are the causing factor of local bench failure and rockfalls. Planner and toppling failures are observed and many wedge failures were also present along the road, due to intersecting discontinuities. Weathering and reduction of joint friction are also driving forces, but the failure is mainly induced by discontinuity orientation. RMR, SMR, and modified GSPI are tabulated in Table 3 for all six locations.

Kinematic analysis suggested that all the locations are susceptible to some kind of failure with different probabilities as shown in Fig. 4. The average probability of failure along the road cut slope is highest for wedge failure with 36.4%, followed by planer failure

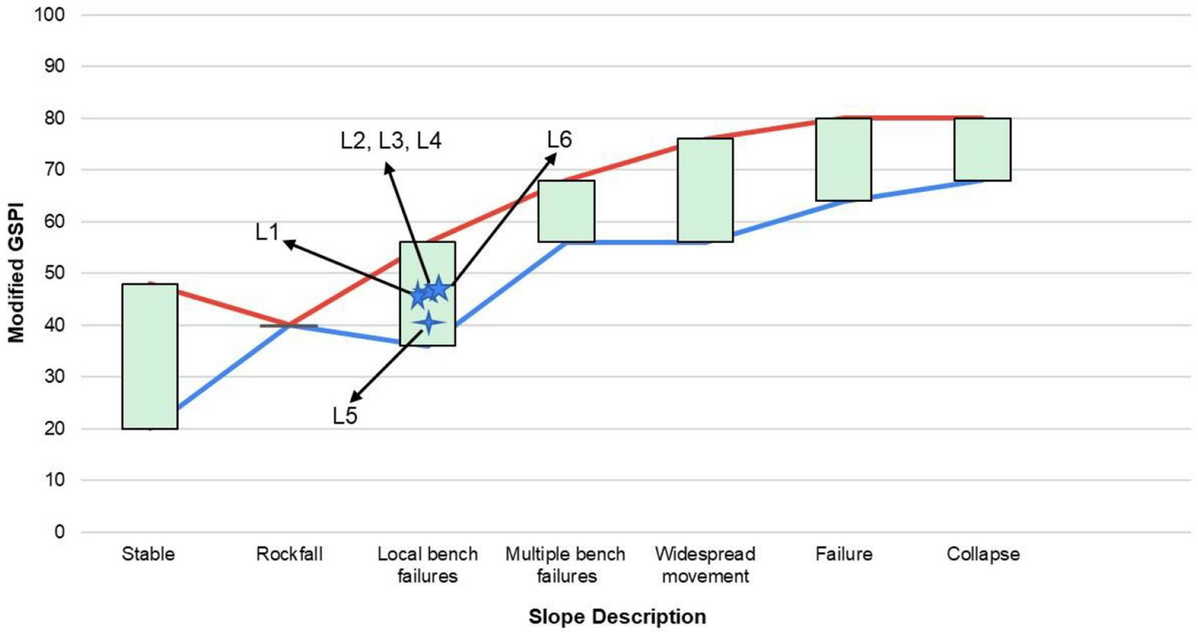

Fig. 12 Floating bar for rating of modified GSPI and slope description (Sullivan 2013)

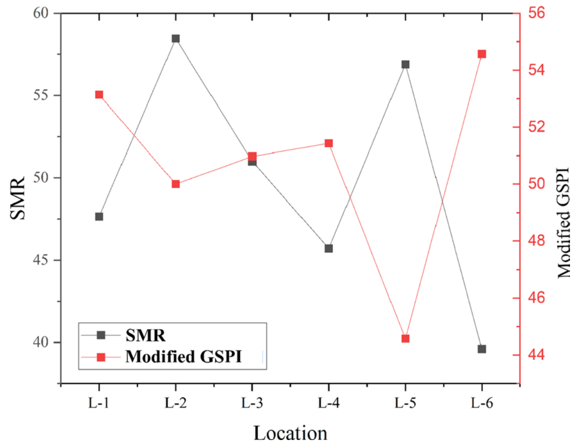

Fig. 13 Detailed correlation of SMR and modified GSPI

Table 3 Ratings of rockmass classification schemes

Location	RMR	SMR	Modified GSPI	Q-Slope	β
L-1	51	47.64	53.14	0.057	33.45
L-2	60	58.46	50.00	0.083	23.38
L-3	57	51	50.97	0.005	53.97
L-4	49	45.7	51.43	0.077	37.72
L-5	62	56.9	44.57	0.062	30.86
L-6	40	39.61	54.57	0.053	54.48

with no limit 27.3%, the direct toppling with 18.2% and flexural toppling and planer failure with limit have equal chances of failure with 9.1% each, shown in Fig. 2. A kinematic analysis of each location with probability and type of failure is given in Table 4.

7 Conclusion

The prime objective of this work is to evaluate the stability of six cut slopes along SH-05A, Markundi Hill, Uttar Pradesh, India. Different rock mass classification schemes and kinematic analysis were employed to identify instability and vulnerability to failure under natural conditions. The petrographic analysis of the scarp sandstone reveals that the framework grains are composed of quartz, while the matrix consists of muscovite. Slake durability indexes are found between 96.49 to 98.83%, suggesting the rocks are less susceptible to weathering. Predominantly, planar and wedge failures are observed in kinematic analysis, whereas some instances show toppling failures too, which are also observed in the field visit. The RMR and GSI yielded nearly identical findings, indicating that the rocks are primarily blocky and disturbed and rated as fair to good in condition. The

Table 4 Kinematic analysis and probability of failure

Location	Number of joints	Planar %	Wedge %	Flexural toppling %	Direct toppling %
L-1	3	33.33	66.67	0.00	33.33
L-2	3	33.33	33.33	0.00	33.33
L-3	3	33.33	33.33	33.33	0.00
L-4	3	0.00	0.00	0.00	33.33
L-5	4	25.00	33.33	0.00	33.33
L-6	10	0.00	0.00	0.00	28.89

quantifiable assessment of slope stability using SMR and modified GSPI approach across various slopes yielded consistent outcomes, showing good agreement. The results indicate that the slopes are partially stable through all methods used in the study, except for location 4. And, it was deemed unstable in both the SMR and modified GSPI analyses. To enhance the empirical findings and determine a stable slope angle during excavation, a Q-slope analysis was performed. Locations 2–6 exhibit a comparable probability of failure as seen in other empirical methods, while location 1 is at the boundary of stable/unstable. Given the partial stability and instability identified through empirical slope analysis, lucrative kinematic analyses were also employed to improve the study of slope stability. The result indicates all the slopes are unstable, location 6 can be stabilized using systematic reinforced shotcrete or exaction of slope and modifying drainage. All the remaining slopes can be stabilized by using nets/anchors and systematic bolting/shotcreting. All the locations need the application of safety measures. The modified GSPI discussed was found to be more robust since it includes larger detail of rockmass properties, without altering the rock class. Since modified GSPI can predict greater types of instabilities, it should be used in conjunction with other classification methods.

The present study yields the following key conclusions:

1. The rock mass exhibits fair quality, in general. However, prominent failure types indicate that intersecting discontinuities primarily drive these instabilities. Field observations and kinematic analysis reveal the same and demonstrate all possible modes of failure, except circular.
2. Various empirical schemes, such as Q-slope, SMR, and GSPI, validate good concordance with kinematic analysis, emphasizing the critical status road cut excavations.
3. In this study, the GSPI is modified by incorporating two highly weighted parameters from SMR. i.e. condition and spacing of discontinuities.
4. Originally, GSPI had a different scale. The modified GSPI, with equal weightage, is now comparable with SMR.
5. GSPI facilitates the identification of a broader spectrum of failures, ranging from stable to collapse conditions. The modified GSPI indicates local bench failure at the studied location in the current study, verified by field observations.
6. The modified GSPI proves effective in identifying various types of failures and will be applied in different environments in conjunction with other classification methods.

Acknowledgements AK would like to thank the Institute of Eminence (IOE), Banaras Hindu University for the seed grant. The authors are grateful to Rocscience, Inc (Canada) for the computation tool, and the Geological Survey of India for maps of the study area.

Authors Contributions Vikas Yadav: Investigation, Data curation, Writing—original draft: Ashutosh Kainthola: Conceptualization, Resources Funding acquisition, Methodology, Writing—original draft: Vishnu HR Pandey: Formal Analysis, Software, Visualization: Gaurav Khushwaha: Formal Analysis, Software, Validation: T.N. Singh: Supervision, Project administration, Writing—review & editing.

Funding This research is support by BHU (Grant No: IOE Seed Grant).

Data Availability All the available data present in this article is generated by the authors themselves.

Declartions

Conflict of interest The authors declare there is no competing interest.

References

Aki K, Richards PG (2002) Quantitative seismology (2nd ed.). University Science Books

Ansari TA, Sharma KM, Singh TN (2019) Empirical slope stability assessment along the road corridor NH-7, in the Lesser Himalayan. Geotech Geol Eng 37:5391–5407. https://doi.org/10.1007/s10706-019-00988-w

Avcı KM, Akgün H, Doyuran V (1999) Assessment of rock slope stability along the proposed Ankara-Pozantı auto road in Turkey. Environ Geol 37(1):137–144. https://doi.org/10.1007/s002540050370

Aydin A, Basu A (2005) The Schmidt hammer in rock material characterization. Eng Geol 81(1):1–14. https://doi.org/10.1016/j.enggeo.2005.06.006

Azarafza M, Koçkar MK, Zhu HH (2022) Correlations of SMR-Qslope data in stability classification of discontinuous rock slope: A modified relationship considering the Iranian data. Geotech Geol Eng 40:1751–1764. https://doi.org/10.1007/s10706-021-01991-w

Bar N, Barton N (2017) The Q-Slope method for rock slope engineering. Rock Mech Rock Eng 50:3307–3322. https://doi.org/10.1007/s00603-017-1305-0

Bartarya SK, Valdiya KS (1998) Landslides and erosion in the catchment of the Gaula River, Kumaun Lesser Himalaya India. Mount Res Dev 9(4):405–419. https://doi.org/10.2307/3673588

Barton N, Bar N (2015) Introducing the Q-slope method and its intended use within civil and mining engineering projects. In: Schubert W, Kluckner A (eds.) Future development of rock mechanics; Proceedings of the ISRM regional symposium, Eurock and 64th geomechanics colloquium, Salzburg, pp. 157–162

Bieniawski ZT (1989) Engineering rock mass classifications: a complete manual for engineers and geologists in mining, civil, and petroleum engineering. Wiley, New York

Bieniawski ZT (1976) Rock mass classification in rock engineering. In: Bieniawski ZT (ed) Symposium Proceedings of Exploration for Rock Engineering, 1, 97–106

Bieniawski ZT (1979) The geomechanics classification in rock engineering applications. In: 4th ISRM congress, Montreux, Switzerland

Brencich A, Bovolenta R, Ghiggi V, Pera D, Redaelli P (2020) Rebound hammer test: an investigation into its reliability in applications on concrete structures. Adv Mater Sci Eng. https://doi.org/10.1155/2020/6450183

Broch E, Franklin JA (1972) The Point-load strength test. Int J Rock Mech Min Sci Geomech Abstr 9:669–676. https://doi.org/10.1016/0148-9062(72)90030-7

Chand K, Koner R (2024) Failure zone identification and slope stability analysis of mine dump based on realistic 3d numerical modeling. Geotech Geol Eng 42:543–560. https://doi.org/10.1007/s10706-023-02588-1

Chaudhary V, Srivastav A, Pandey VHR et al (2022) Physico-mechanical characteristics of Vindhyan sandstone, India. J Inst Eng India Ser D 103:295–302. https://doi.org/10.1007/s40033-021-00301-1

Chiwaye H, Stacey TR (2010) A comparison of limit equilibrium and numerical modelling approaches to risk analysis for open pit mining. J South Afr Inst Min Metall 110:571–580

Das S, Pandit K, Sarkar S, Kanungo DP (2024) Stability and hazard assessment of the progressive zero landslide in the Kalimpong region of Darjeeling Himalaya, India. Geotech Geol Eng 42:1693–1709. https://doi.org/10.1007/s10706-023-02641-z

Deere D (1963) Technical description of rock cores for engineering purposes. Rock Mech Eng Geol 1(1):17–22

Dikshit A, Sarkar R, Pradhan B, Segoni S, Alamri AM (2020) Rainfall induced landslide studies in Indian Himalayan region: a critical review. Appl Sci 10:2466. https://doi.org/10.3390/app10072466

Doumbouya L, Guan CS, Bowa VM (2020) Influence of rainfall patterns on the slope stability of the Lumwana (the Malundwe) Open Pit. Geotech Geol Eng 38:1337–1346. https://doi.org/10.1007/s10706-019-01094-7

Eberhardt E (2023) Rock slope stability analysis-utilization of advanced numerical techniques

Franklin JA, Chandra R (1972) The slake-durability test. Int J Rock Mech Min Sci Geomech Abstr 9(3):325–328. https://doi.org/10.1016/0148-9062(72)90001-0

Fraser-Harris A, Lightbody A, Edlmann K, Elphick S, Couples GD, Sauter M, McDermott CI (2020) Sampling and preparation of c200 mm diameter cylindrical rock samples for geomechanical experiments. Int J Rock Mech Min Sci 128:104233. https://doi.org/10.1016/j.ijrmms.2020.104233

Geological Survey of India (2023) Bhukosh. Geological Survey of India. https://bhukosh.gsi.gov.in/Bhukosh/Public Accessed 2023

Goel RK, Singh B (2011) Engineering rock mass classification: tunnelling, foundations, and landslides. Elsevier, Amsterdam. ISBN: 9780128103647

Gordan B, Jahed AD, Hajihassani M, Monjezi M (2015) Prediction of seismic slope stability through combination of particle swarm optimization and neural network. Eng Comput. https://doi.org/10.1007/s00366-015-0400-7

Hassan B, Hani M (2017) Application of rock mass classification systems to rock slope stability assessment: a case study. J Rock Mech Geotech Eng 9(6):993–1009. https://doi.org/10.1016/j.jrmge.2017.07.007

Hoek E, Bray J (1981) Rock slope engineering. The Institution of Mining and Metallurgy, London

Hoek E, Brown ET (1997) Practical estimates of rock mass strength. Int J Rock Mech Min Sci 34(8):1165–1186. https://doi.org/10.1016/S1365-1609(97)80069-X

Hoek E, Kaiser PK, Bawden WF (1995) Support of underground excavations in hard rock Rotterdam: A.A. Balkema. pp. 58–65

Hong K, Han E, Kang K (2017) Determination of geological strength index of jointed rock mass based on image processing. J Rock Mech Geotech Eng 9(4):702–708. https://doi.org/10.1016/j.jrmge.2017.05.001

Kainthola A, Sharma V, Pandey VHR, Jayal T, Singh M, Srivastav A, Singh PK, Prashant K, Ray C, Singh TN (2021) Hill slope stability examination along Lower Tons valley, Garhwal Himalayas, India. Geomat Nat Haz Risk 12(1):900–921. https://doi.org/10.1080/19475705.2021.1906758

Kainthola A, Pandey VHR, Singh PK, Singh TN (2023) Stability assessment of Markundi Hills using Q-slope, SMR and simulation tools. In: Thambidurai P, Singh TN (eds) Landslides: detection, prediction and monitoring. Springer, Cham. https://doi.org/10.1007/978-3-031-23859-8_4

Kumar S, Pandey HK, Singh PK, Venkatesh K (2019) Demarcation of probable failure zones based on SMR and kinematic analysis. Geomat Nat Haz Risk 10(1):1793–1804. https://doi.org/10.1080/19475705.2019.1618399

Li Z, Wang M, Yu S, Liu J (2024) Effects of the root's distribution on the stability of slope. Geotech Geol Eng 42:1009–1019. https://doi.org/10.1007/s10706-023-02601-7

Małkowski P, Ostrowski L, Brodny J (2018) Analysis of Young's modulus for carboniferous sedimentary rocks and its relationship with uniaxial compressive strength using different methods of modulus determination. J Sustain Min. https://doi.org/10.1016/j.jsm.2018.07.002

Marinos P, Hoek E (2000) GSI: A geologically friendly tool for rock mass strength estimation. In: ISRM international symposium. International Society for Rock Mechanics

Marinos V, Carter TG (2018) Maintaining geological reality in the application of GSI for the design of engineering structures in rock. Eng Geol 239:282–297. https://doi.org/10.1016/j.enggeo.2018.03.022

Mishra M, Sen S (2011) Geochemical signatures for the grain size variation in the siliciclastics of Kaimur Group, Vindhyan Supergroup from Markundi ghat, Sonbhadra district, (U.P.) India. Geochem Int 49:274–290. https://doi.org/10.1134/S0016702911010071

Molina O, Vilarrasa V, Zeidouni M (2017) Geologic carbon storage for shale gas recovery. Energy Procedia 114:5748–5760

Monjezi M, Singh TN (2000) Slope instability in an opencast mine. Coal Int 8:145–147

Monjezi M, Nourali HR, Singh TN (2011) Study of the effect of rainfall on slope stability—a numerical approach. Indian Landslides 4(1):13–18

Norbury D (1986) The point load test. Geol Soc Lond Eng Geol Spec Publ 2:325–329. https://doi.org/10.1144/GSL.1986.002.01.56

Palmstrom A (1974) Characterization of jointing density and the quality of rock masses. Internal report, A.B. Berdal, Norway, 26 p (in Norwegian)

Pandey VHR, Kainthola A, Sharma V et al (2022) Deep learning models for large-scale slope instability examination in Western Uttarakhand India. Environ Earth Sci 81:487. https://doi.org/10.1007/s12665-022-10590-8

Panthee S, Dulal S, Pandey VHR et al (2023) Engineering geological characteristics and failure mechanics of Jure rock avalanche. Nepal Geoenviron Disasters 10:25. https://doi.org/10.1186/s40677-023-00256-3

Park HJ, Lee JH, Kim KM, Um JG (2015) Assessment of rock slope stability using GIS-based probabilistic kinematic analysis. Eng Geol 203:56–69. https://doi.org/10.1016/j.enggeo.2015.08.021

Peng Y, Gao Y, Xie Y et al (2024) Effect of joint angle on the failure behavior of rock-like specimens under unilateral restrained compression. Geotech Geol Eng. https://doi.org/10.1007/s10706-024-02844-y

Rawat DS, Yadav V, Naithani AK et al (2024) Assessment of discontinuity related instability potential in a surge pool cavern: kinematic and distinct element approach. Discov Geosci 2:12. https://doi.org/10.1007/s44288-024-00013-5

Rehman I, Zhang AU, AlQahtani G, Janjuhah SA, Hussain HT, Shah HU (2023) Geotechnical assessment of rock slope stability using kinematic and limit equilibrium analysis for safety evaluation. Water 15:1924. https://doi.org/10.3390/w15101924

Romana MR (1993) A geomechanical classification for slopes: slope mass rating. Rock Test Site Charact 3(1):575–600

Romana MR (1985) New adjustment ratings for application of Bieniawski classification to slopes. In: Proceedings of the international symposium on the role of rock mechanics in excavations for mining and civil works. International Society of Rock Mechanics, Zacatecas, pp. 49–53

Sardana S, Verma AK, Singh A (2019) Comparative analysis of rockmass characterization techniques for the stability prediction of road cut slopes along NH-44A, Mizoram India B. Eng Geol Environ 78(8):5977–5989. https://doi.org/10.1007/s10064-019-01493-3

Shang J, West L, Hencher S, Zhao Z (2018) Geological discontinuity persistence: implications and quantification. Eng Geol. https://doi.org/10.1016/j.enggeo.2018.05.010

Shearer PM (2009) Introduction to Seismology (2nd ed.). Cambridge University Press

Singh TN, Monjezi M (2000) Slope stability study in jointed rockmass—a numerical approach. Min Eng Jl 1(10):12–13

Sonmez H, Ulusay R (2002) A discussion on the Hoek-Brown failure criterion and suggested modifications to the criterion verified by slope stability case studies. Yerbilimleri 26:77–99

Starkel L (1972) The role of catastrophic rainfall in the shaping of the relief of the Lower Himalaya (Darjeeling Hills). Geogr Pol 21:103–160

Sullivan TD (2013) Global slope performance index, in PM Dight (ed.), Slope Stability 2013: Proceedings of the 2013 International Symposium on Slope Stability in Open Pit Mining and Civil Engineering, Australian Centre for Geomechanics, Perth, pp. 55–80. https://doi.org/10.36487/ACG_rep/1308_0.4_Sullivan

Tiwari VN, Pandey VHR, Kainthola A et al (2020) Assessment of Karmi landslide zone, Bageshwar, Uttarakhand, India. J Geol Soc India 96:385–393. https://doi.org/10.1007/s12594-020-1567-0

Virdi NS, Sah MP, Bartarya SK (2015) Project Report: landslide hazard zonation in the Beas and Satluj valleys of Himachal Pradesh, Phase-I Satluj Valley. Wadia Institute of Himalayan Geology, Technical Report, pp.132

West I, Walton G, Gonzalez-Fernandez M et al (2024) Mechanical behavior of intact and increasingly jointed marble laboratory specimens. Geotech Geol Eng. https://doi.org/10.1007/s10706-024-02815-3

Yoon WS, Jeong UJ, Kim JH (2002) Kinematic analysis for sliding failure of multi-faced rock slopes. Eng Geol 67(1–2):51–61. https://doi.org/10.1016/S0013-7952(02)00144-8